Parameters Analysis of Line Segment Fabrication on Near-Field Photolithography

Ching-Been Yang, Hsiu-Lu Chiang, Jaw-Ren Lin*

Department of Mechanical Engineering, Nanya Institute of Technology
*been@nanya.edu.tw

Abstract -This paper proposes the integral formula of exposure energy density during the movement of work piece to investigate the exposure energy distribution on the photoresist surface. The photoresist was divided into finite nodes to combine the integral formulas of exposure energy density to calculate the relative concentration variation of the photoactive compound (PAC) at each finite node of photoresist interior layer. This paper further combines with Mack's development model and calculates the average full-width at half maximum (FWHM) of near field photolithography. This study conducted sensitivity analysis to determine how adjusting groups of control parameters influences full-width at half maximum (FWHM) and working depth (Hmax). Group A, in which the probe aperture was the adjusted parameter, had the most influence, followed by Group B, in which exposure energy/μm was the adjusted parameter, and Group C, in which development time was the adjusted parameter.

Keywords: Near field photolithography, Power density, FWHM, sensitivity analysis

I. INTRODUCTION

This paper attempts to build up a line segment fabrication model for near field photolithography to carry out simulation and analysis so as to understand the process of the near field photolithography.

Betzig et al. [1] indicated that the traditional light diffraction limit, overcome by near-field photolithography technology, is proved theoretically and high-level resolution images are obtained. The following year, Betzig et al. [2] indicated that super-resolution imaging was obtained by using collection-mode near-field scanning optical microscopy. Balanis [3] mentioned in his text the near zone radiation formulas of electromagnetic theorem.

Regarding the analytical study of optical fiber probe, Lin and Yang [4] analyzes the near field power density distribution for different models of an optical fiber probe. Naber et al. [5] used the argo-ion laser at a wavelength of 455 nm to make a fabrication line at the FWHM between 80 and 150 nm.

Regarding the exposure theorem of photolithography, Dill [6] proposed in the photoresist exposure model to calculate the concentration variation of photoactive compound (PAC) after exposure in 1975. Later on, in 1986 Babu [7] found the exact solution for Dill's partial differential equation of photoresist exposure, greatly increases the applicability of Dill's photoresist exposure model.

As to the development theory of photolithography, Mack [8] studied the physical and chemical reactions of the development process. A kinetic model of development process to describe development mechanisms has been proposed, and acquired the expression for development rate. Lin and Yang [9] first combined radiation-field theory, Dill's exposure model and Mack's development model to analyze the process of near field photolithography fabrication.

This paper proposes the integral formula of the exposure energy density during the movement of workpiece so as to analyze the exposure distribution on photoresist surface. Dividing photoresist into finite nodes, this paper combines the integral formulas of exposure power density, and calculates the PAC relative concentration variation at each finite node of photoresist interior layer after exposure. Finally, this paper further combines with Mack's development model and calculates the development rate after photoresist development, the average FWHM of near field photolithography and the fabrication profile. This study conducted sensitivity analysis to determine how adjusting groups of control parameters influences full-width at half maximum (FWHM) and working depth (Hmax).

II. LINE SEGMENT FABRICATION MODEL OF NEAR FIELD PHOTOLITHOGRAPHY

The line fabrication model of the near field photolithography combines the near zone radiation theory of electromagnetism, Dill's photoresist exposure model, and Mack's photoresist development model.

A. Power Density for Aluminum-coated Probe

Lin and Yang [9] utilized $\vec{E}_a$ and $\vec{H}_a$ to represent the electrical field and magnetic field of the emission zone of the aluminum-coated fiber probe. The electric field of the observation point can be expressed as

$$\vec{E}_F\ (x,y,z)=\frac{1}{4\pi}\iint_S(\vec{n}_R\times\vec{M}_S)\frac{1+j\beta R}{R^2}e^{-j\beta R}ds' \tag{1}$$

In which $\vec{M}_S$ is the magnetic current source, $\vec{n}_R$ is a unit vector directed along the line joining any point of the surface and observation point. By using Maxwell's equation, the magnetic field equation of the observation point can be expressed as:

$$\vec{H}_F=-\frac{1}{j\omega\mu_0}\nabla\times\vec{E}_F \tag{2}$$

Here, μ_0 represents the permeability of near field space. The maximum power density of the observation point acquired through normalization is 1. Then the normalized power density of the observation point can be acquired through the following equation [9]:

$$I_{nor}(x,y,z)=\frac{1}{2}\mathrm{Re}\{\ \vec{E}_F\times\vec{H}_F^{\ *}\ \} \tag{3}$$

in which, $I_{nor}(x,y,z)$ denotes the normalized power density of the observation point, $\vec{E}_F$ the electric field of the observation point caused by the magnetic current source $\vec{M}_S$, $\vec{H}_F$ the magnetic field of the observation point caused by the magnetic current source $\vec{M}_S$, and * the complex conjugate.

To calculate the density of energy absorbed by the photoresist surface during point photolithography exposure, Lin and Yang [9] utilized the exposure energy density formula of a static fixed point as follows:

$$E_P((x_P, y_P, h=0), t) = I_P(x_P, y_P, h=0) \times t \quad (4)$$

where $E_P((x_P, y_P, h=0), t)$ is the density of energy absorbed by the photoresist surface at exposure time t during point fabrication, and t the exposure time.

1) Exposure energy density distribution of the line segment fabrication model of near field photolithography

If an optical fiber probe with a radius of ρ_0 is used to carry out line segment photolithographic fabrication, the optical fiber probe scans the workpiece rightward for a length L with a constant velocity V. Also, during line segment fabrication, the energy density of each node of the photoresist surface is either the sum of the entire exposure power density of the accumulated point fabrication, or the sum of the partial exposure power density of the accumulated point fabrication. Based on the given condition, Lin and Yang [10] divides the exposure energy density area of line segment fabrication into the following five zones:

Zone 1: ($-2\rho_0 \le x_L < 0$)

$$E_L(x_L, y_L, h=0) = \frac{\int_{-2\rho_0}^{-l'} I_P(x_P, y_P, h=0) dx_P}{V} \quad 0 \le l' < 2\rho_0,\ y_P = y_L,\ x_L = -l' \quad (5a)$$

Zone 2: ($0 \le x_L < 2\rho_0$)

$$E_L(x_L, y_L, h=0) = \frac{\int_{-2\rho_0}^{l} I_P(x_P, y_P, h=0) dx_P}{V} \quad l = x_L,\ y_P = y_L,\ 0 \le x_L < 2\rho_0 \quad (5b)$$

Zone 3: ($2\rho_0 \le x_L \le L - 2\rho_0$)

$$E_L(x_L, y_L, h=0) = \frac{\int_{-2\rho_0}^{2\rho_0} I_P(x_P, y_P, h=0) dx_P}{V} \quad y_P = y_L \quad (5c)$$

Zone 4: ($L - 2\rho_0 < x_L < L$)

$$E_L(x_L, y_L, h=0) = \frac{\int_{-l'}^{2\rho_0} I_P(x_P, y_P, h=0) dx_P}{V} \quad l' = L - x_L,\ y_P = y_L, L - 2\rho_0 \le x_L \le L \quad (5d)$$

Zone 5: ($L \le x_L \le L + 2\rho_0$)

$$E_L(x_L, y_L, h=0) = \frac{\int_{l}^{2\rho_0} I_P(x_P, y_P, h=0) dx_P}{V} \quad l = x_L - L,\ y_P = y_L, L \le x_L \le L + 2\rho_0 \quad (5e)$$

B. Analysis of photoresist exposure model

This paper was employed photoresist exposure model suggested by Dill [7]. According to the various nodes of the coordinate $((x_L, y_L), h)$ being divided from the photoresist interior layer, this paper revises Dill's photoresist exposure model according to the following equations:

$$\frac{\partial I_{PR}((x_L, y_L), h, t)}{\partial h} = -I_{PR}((x_L, y_L), h, t) \times \left[A \times M_{PR}((x_L, y_L), h, t) + B\right] \quad (6a)$$

$$\frac{\partial M_{PR}((x_L, y_L), h, t)}{\partial t} = -I_{PR}((x_L, y_L), h, t) \times M_{PR}((x_L, y_L), h, t) \times C \quad (6b)$$

In the above formula, $I_{PR}((x_L, y_L), h, t)$ represents the laser intensity at time t and exposure depth h $M_{PR}((x_L, y_L), h, t)$ represents the relative concentration of PAC at time t and exposure depth h, t is the exposure time

In Equation (6a) and (6b), A, B, and C are called Dill A, B, and C parameters.

The photoresist exposure model proposed by Dill is a partial differential equation, whose exact solution is acquired by Babu as follows [8]:

$$h = \int_{g(t)}^{M_{PR}((x_L, y_L), h, t)} \frac{1}{h' \times [A \times (1 - h') - B \times \ln h']} dh' \quad (7)$$

here, g(t) is just $M_{PR}((x_L, y_L), h = 0, t)$ when h=0. Hence,

$$g(t) = M_{PR}((x_L, y_L), h = 0, t) = e^{-E_L((x_L, y_L), h=0, t) \times C} \quad (8)$$

where $E_L((x, y), h = 0, t)$ is exposure energy density at the photoresist surface, of which the $M_{PR}((x_L, y_L), h, t)$ of each node inside the photoresist layer must be acquired by substituting exposure energy density of pattern fabrication into $E_L((x_L, y_L), h = 0, t)$ in Eq. (8).

C. Analysis of photoresist development model

According to the photoresist interior layer, this paper divided the photoresist into different nodes of coordinate $((x_L, y_L), h)$, and revises Mack's development model as the following formula [9]:

$$R_{bulk}((x_L, y_L), h, t) = R_{\max} \times \frac{(\alpha + 1) \times (1 - M_{PR}((x_L, y_L), h, t))^n}{\alpha + (1 - M_{PR}((x_L, y_L), h, t))^n} + R_{\min} \quad (9)$$

in which:

$$\alpha = \frac{n+1}{n-1}(1 - M_{th})^n \quad (10)$$

$R_{bulk}((x_L, y_L), h, t)$: photoresist development rate

$R_{\max}$: photoresist development rate after exposure for a long time

$R_{\min}$: photoresist development rate before exposure

M_{th} : threshold of PAC relative concentration

n: selection factor

Normally the cross-linking reaction of resin occurs on the photoresist surface due to the baking at high temperature, thus creating induction effect to the photoresist surface and the slowdown of development rate near the photoresist surface. This paper refers to the photoresist data of Shipley Company's SPR3001 model. The critical depth of this induction effect is 10 nm. Therefore, the photoresist development rate at $0 \le h \le 10$ has to be like [9]:

$$R_{10}((x_L, y_L), h, t) = R_{bulk}((x_L, y_L), h, t) \times (1 - (1 - R_0) \times e^{-\gamma h}) \quad (11)$$

in which,

R_{10}: photoresist development rate at the depth of $0 \le h \le 10$

γ: a constant satisfying the continuity between R_{bulk} and R_{10}

When the exposure time t is known, the development rate $R_{bulk}((x_L, y_L), h, t)$ of each node in the interior of photoresist can be calculated from Equation (9). Since the exposure time t is already known, the recurrence relation can be simplified as $R_{bulk}((x_L, y_L), h)$. Similarly, one can obtain the recurrence relation $R_{10}((x_L, y_L), h)$ in Equation (11). Furthermore,

$$R((x_L, y_L), h) = \frac{dh}{dt_d} \tag{12}$$

in which, R denotes the development rate and t_d denotes the development time. Therefore,

$$\int_0^H \frac{dh}{R_{10}((x_L, y_L), h)} = \int_0^{t_d} d\tau \tag{13a}$$

$$\int_{h_{crit}}^H \frac{dh}{R_{bulk}((x_L, y_L), h)} = \int_{t_{dcritt}}^{t_d} d\tau \tag{13b}$$

where H is development depth. According to development time, the depth H of the photoresist at each node (x_L, y_L) being developed can be determined by Eq. (13a) or Eq. (13b). Afterwards, the development depth, H, of all (x_L, y_L) coordinates of the entire photoresist can be depicted. Finally, development depth, H, of all photoresist coordinates of (x_L, y_L) are connected to form the profile of the photoresist after development, and the values of FWHM can be determined with this profile.

III. RESULTS AND DISCUSSION OF SENSITIVITY ANALYSIS

A. Control Factor level of sensitivity analysis

Although the process parameters of the near field photolithography experiment include four parameters, namely, the probe aperture, exposure power, exposure velocity and development time, the exposure power of probe cannot be easily controlled and the range of adjustment is limited. Therefore, having coupled with the laser coupler in the experiment, each probe shall have its fixed value maintained and not adjusted anymore. It implies that the exposure power is not included in the adjustment parameters of the experiment, and the exposure velocity is taken as the adjustment parameter for controlling the exposure energy per unit length. This paper takes three parameters, i.e., 1.probe aperture (PA), 2.exposure energy per unit length (ee), and 3.development time (DT), as the control factors of the near field photolithographic line fabrication. Each control factor has three levels, and the control factors and their levels are shown in Table 1.

B. Sensitivity analysis

The parameters employed in the simulation experiment for line segment fabrication of near-field photolithography are as follows: Dill's A=3.393×10^{-4} 1/nm, B=7.885×10^{-4} 1/nm, and C=1398.1 nm^2/nJ; R_{max}=132.26 nm/s, R_{min}=0.029 nm/s, M_{th} = 0.5, w = 0.69, and z= 5 [10]. The sensitivity analysis is described in terms of three groups with different adjusted parameters. In Group A, the two parameters, exposure energy/μm and development time, were fixed, and probe aperture was adjusted. In Group B, probe aperture and development time were fixed while exposure energy/μm was adjusted. Finally, in Group C, probe aperture and exposure energy/μm were fixed and development time was adjusted. The control parameters in the sensitivity analysis were substituted into the line segment fabrication model of near-field photolithography in a controlled manner. The results are displayed in Table 2. The influence of these three groups of control parameters on the fabrication procedure is discussed as follows:

Group A: Variation in probe aperture

The purpose of this group was to analyze the influence of probe aperture on the fabrication procedure. The other two parameters, exposure energy/μm and exposure time, were fixed at 30 nJ/μm and 1.5 s, respectively. Figure 1 shows the power density distribution of the optical fiber probe in Group A1 (PA=140 nm; ee =30 nJ/μm; DT=1.5 sec); Fig. 2 displays the fabrication profile of Group A1. Figures 3 and 4 present the influence of the control parameters in the sensitivity analysis on FWHM and Hmax, respectively. As seen in Fig. 3, a reduction in probe aperture decreases FWHM. The data in Fig. 4 show that an increase in probe aperture in the sensitivity analysis also results in a decrease in Hmax.

Group B: Variation in exposure energy/μm

Among the parameters of this group, exposure energy/μm was adjusted while the other two parameters, probe aperture and development time, were fixed at 180 nm and 1.5 s, respectively. Figures 3 and 4 indicate that FWHM and Hmax both increase with exposure energy/μm.

Group C: Variation in development time

In this group, development time was set as the adjusted parameter and the other two parameters, probe aperture and exposure energy/μm, were fixed at 180 nm and 30 nJ/μm, respectively. The purpose of these settings was to explore the influence of development time on the fabrication procedure. Figure 3 reveals that no relationship is evident between FWHM and development time in the sensitivity analysis. Figure 4 shows that Hmax and exposure time are proportional to one another; therefore, Hmax increases with development time.

In terms of the relative influence that control parameters have on FWHM in the sensitivity analysis, Fig. 3 shows that among the three groups of parameter settings, Group A, in which the probe aperture was the adjusted parameter, had the most influence, followed by Group B, in which exposure energy/μm was the adjusted parameter, and Group C, in which development time was the adjusted parameter. These results support the findings of Lin and Yang [11], who employed the Taguchi method to investigate the same effects. This demonstrates that the analysis method developed in this study is reasonable and feasible.

Figure 4 shows the influence of the three groups of parameters on Hmax in the sensitivity analysis (a steeper slope indicates a larger influence). Among the three groups, Group A has the largest influence, followed by Group C and Group B.

IV. CONCLUSIONS

This paper revises the exposure energy density formula of the near field photolithography model at static fixed point, and proposes the integral formula of exposure energy density during the work piece moving so as to analyze and investigate the exposure energy distribution of photoresist surface. Meanwhile, in order to acquire the PAC relative concentration variation at each finite node of photoresist interior layer, this paper divides the photoresist into finite nodes, and combines the integral formulas of exposure energy density. This paper further calculates the PAC relative concentration variation at each finite node of photoresist interior layer after photoresist exposure. Finally, this paper calculates the average full-width at half maximum (FWHM) of fabrication after photoresist development as well as the fabrication profile. This study employed sensitivity analysis to determine the influence of various combinations of control parameters on FWHM and Hmax. Group A, in which probe aperture was the adjusted parameter, was the most sensitive, followed by Group C, in which exposure energy/µm was the adjusted parameter, and Group C, in which development time was the adjusted parameter. In terms of the influence of the three groups of parameters on Hmax in the sensitivity analysis, Group A had the largest influence among the three groups, followed by Group C, and Group B.

REFERENCES

[1] E. Betzig, A. Harootunian, A. Lewis, M. Isaacson, "Near-field diffraction by a slit: implication for super resolution microscopy," *Applied Optics*, 25 (1986) 1890-1900.

[2] E. Betzig, M. Isaacson, A. Lewis, "Collection mode near-field scanning optical microscopy," *Applied Physics Letters*, 51 (1987) 2088-2090.

[3] Balanis, C. A., *Advanced engineering electromagnetic*, John Wiley & Sons, Inc., (1989).

[4] Z. C. Lin, C. B. Yang, "The near-field power density distribution characteristics for different type optical fiber probes," *International Journal of Advanced Manufacturing Technology*, 26 (2005) 1289-1297.

[5] A. Naber, H. Kock, H. Fuchs, "High-resolution lithography with near-field optical microscopy," *Scanning*, 18 (1996) 567-571.

[6] F. H. Dill, W. P. Hornberger, P. S. Hauge, J. M. Shaw, "Characterization of positive photoresist," *IEEE Transactions on Electron Devices*, 22 (1975) 445-452.

[7] S. V. Babu, E. Barouch, "Exact solution of Dill's model equation for positive photoresist kinetics," *IEEE Electron Devices Letters*, EDL-7 (1986) 252-253.

[8] C. A. Mack, "Development of positive photoresists," *The* Journal of The Electrochemical Society, 134 (1987) 148-152.

[9] Z. C. Lin, C. B. Yang, "Analysis of point-fabrication model for nanometer-scale near field photolithography with experimental study," *Scanning*, 28 (2006) 32-41.

[10] Z. C. Lin, C. B. Yang, "Line segment fabrication model analysis of near field photolithography," *Proceedings of the Institution of Mechanical Engineers, Part B: Journal of Engineering Manufacture*, 223 (2009) 145-154.

[11] Z. C. Lin, C. B. Yang, "Combining the Taguchi method with an artificial neural network to construct a prediction model of near field photolithography experiments," *Proceedings of the Institution of Mechanical Engineers, Part C, Journal of Mechanical Engineering Science*, 224 (2010) 2223-2233.

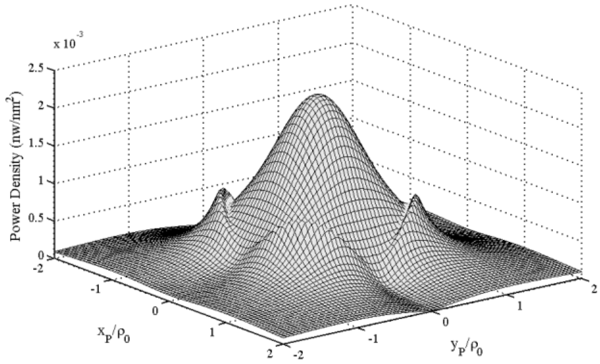

Fig. 1 Power density distribution of optical fiber probe in Group A1

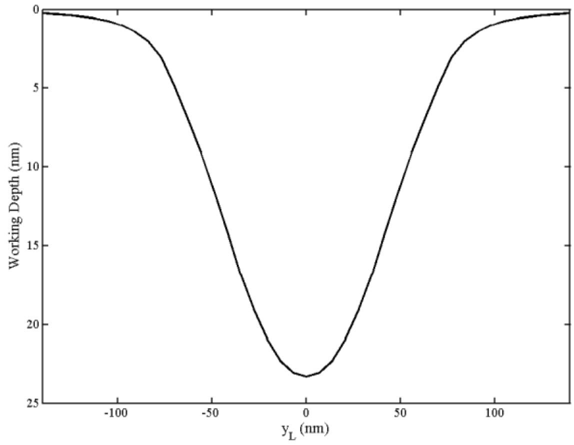

Fig. 2 Fabrication profile of Group A1

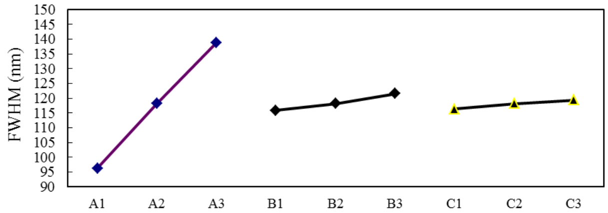

Fig. 3 Influence of control parameters on FWHM in sensitivity analysis

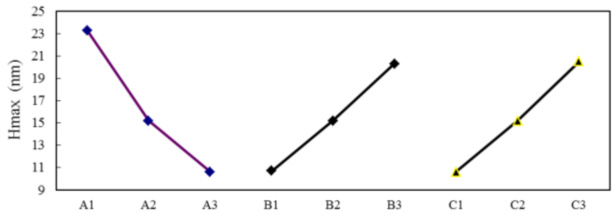

Fig. 4 Influence of control parameters on Hmax in sensitivity analysis

Table 1 Control factors and their levels in the sensitivity analysis

Control factor	1. probe aperture PA(nm)	2.exposure energy/μm ee (nJ/μm)	3.development time DT(sec)
level 1	140	25	1
level 2	180	30	1.5
level 3	220	35	2

Table 2 Simulation results of sensitivity analysis

Group	1. probe aperture PA(nm)	2. exposure energy/μm ee (nJ/μm)	3. development time DT(sec)	FWHM (nm)	Hmax (nm)
A1	140	30	1.5	96.3	23.3
A2	180	30	1.5	118.2	15.2
A3	220	30	1.5	138.9	10.6
B1	180	25	1.5	115.9	10.7
B2	180	30	1.5	118.2	15.2
B3	180	35	1.5	121.5	20.3
C1	180	30	1	116.4	10.6
C2	180	30	1.5	118.2	15.2
C3	180	30	2	119.4	20.5